SUPPORTING INFORMATION

Beneficial effect of cerium excess on the *in-situ* grown $Sr_{0.86}Ce_{0.14}FeO_3$-CeO_2 thermocatalysts for the degradation of Bisphenol A

Martin B. Østergaard[1,*], Francesca Deganello[2,*], Valeria La Parola[2], Leonarda F. Liotta[2], Vittorio Boffa[1],

Mads K. Jørgensen[1]

[1]Center for Membrane Technology, Department of Chemistry and Bioscience, Aalborg University, 9220 Aalborg East,

Denmark

[2]Instituto per lo Studio dei Materiali Nanostrutturati, Consiglio Nazionale delle Ricerche, Via Ugo La Malfa 153,

90146, Palermo, Italy

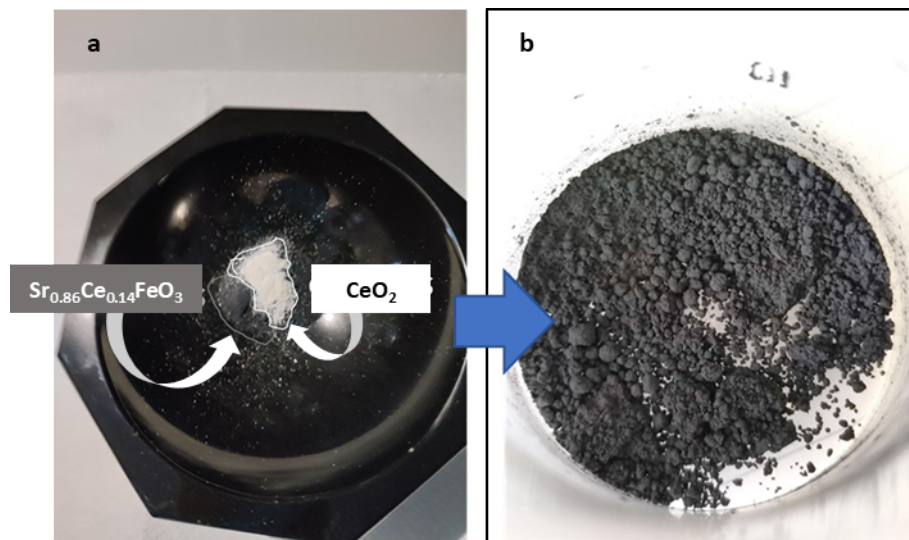*Correspondence: mbo@bio.aau.dk (M.B.Ø.), francesca.deganello@cnr.it (F.D.)

Figure S1. Pictures of the preparation of the mechanical mixture MM between $Sr_{0.86}Ce_{0.14}FeO_3$ (*Ce0*) and CeO_2 before mixing (a) and after mixing (b)
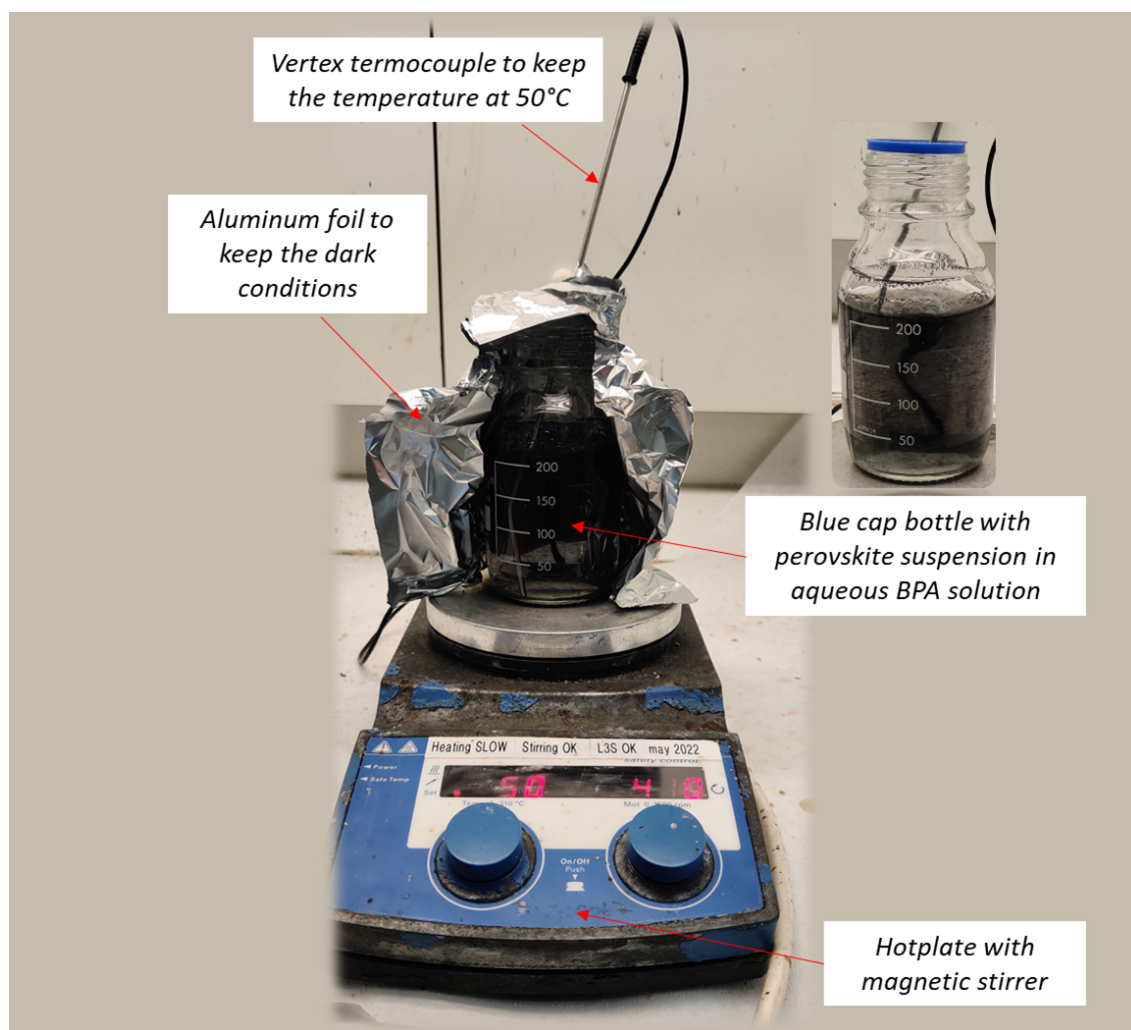
Figure S2. Pictorial description of the thermocatalytic batch experiment.

Table S1. Main structural results obtained from Rietveld refinement of the XRD data with relative standard deviations and reliability factors: phase composition of the powders and space group, unit cell lengths, cell volume, crystallite size,

Sample name	Phase Composition (wt%)	Structure type	Cell Lenghts (Å)	Cell Volume (Å^3)	Crystallite Size (nm)	Microstrain° (unitless)	Reliability Factors
Ce0	P (100)	P m -3 m	3.88454 ± 0.0007	58.616 ± 0.003	369 ± 31	3023 ± 100	GOF* = 1.43 wR§ = 8.49%
Ce5	P (96.2 ± 0.7) F (3.8 ± 0.1)	P4/mmm F m -3 m	3.8864 ± 0.0001 3.8777 ± 0.0002 5.4111 ± 0.0006	58.570 ± 0.005 158.44 ± 0.05	315 ± 35 69 ± 10	3825 ± 164 863 ± 970	GOF = 1.55 wR = 9.71%
Ce10	P (93.2 ± 0.6) F (6.8 ± 0.1)	P4/mmm F m -3 m	3.8887 ± 0.0001 3.8799 ± 0.0002 5.4112 ± 0.0003	58.673 ± 0.005 158.45 ± 0.03	237 ± 20 76 ± 6	3990± 169 1404 ± 505	GOF = 1.47 wR = 8.91%
Ce15	P (89.4 ± 0.6) F (10.6 ± 0.1)	P4/mmm F m -3 m	3.8892 ± 0.0001 3.8799 ± 0.0002 5.4133 ± 0.0003	58.688 ± 0.005 158.63 ± 0.02	432 ± 75 81 ± 6	5240± 193 2258 ± 398	GOF = 1.47 wR = 8.74%
CeO$_2$	F (100)	F m -3 m	5.41177± 0.00007	158.496± 0.006	87 ± 1	637± 62	GOF = 1.20 wR = 8.11%
MM	P (89.47 ± 0.5) F (10.5 ± 0.1)	P m -3 m F m -3 m	3.88535 ± 0.00006 5.4116 ± 0.0002	58.653 ± 0.003 158.48 ± 0.01	352 ± 28 76 ± 3	2920 ± 99 318 ± 247	GOF = 1.29 wR = 7.64%

microstrain of the $Sr_{0.86}Ce_{0.14}FeO_3$ perovskite (P) and CeO$_2$ fluorite (F) phases.

° Microstrain ($10^6 \cdot \Delta d/d$), where d is the distance between symmetry planes and is related to the 2θ angle through the Bragg equation

* GOF= sum[(Iobs-Icalc)/sigma)^2] normalized by the degrees of freedom, which is nobs-nvar, where n is the number of parameters and nvar is the number of refined parameters. It is often called also reduced χ^2

§ wR is the weighted profile R factor and is calculated directly from the square root of the quantity minimized, scaled by the weighted intensities. It is often called also R_{wp}.
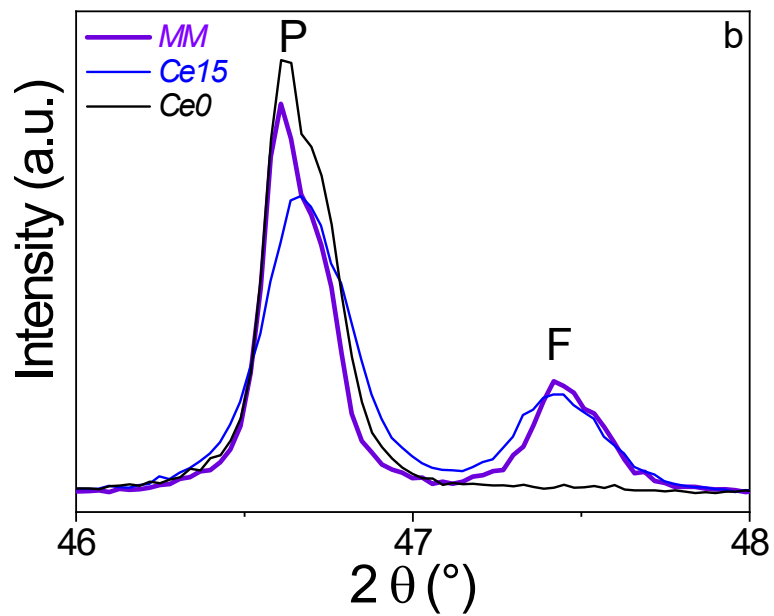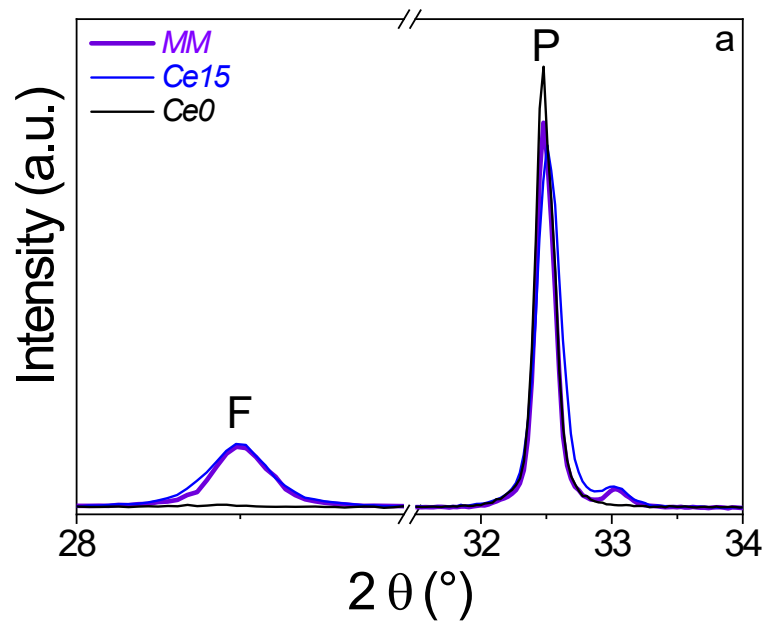
Figure S3. Comparison between XRD pattern of the mechanical mixture, the powder with no cerium excess (*Ce0*) and the powder with the maximum amount of cerium excess (*Ce15*). P and F indicates the perovskite phase and fluorite ceria phase, respectively.

Table S2. Binding Energy (eV) and, in parenthesis, the relative atomic percentages and speciation of the O1s, Fe2p3/2 and Sr3d5/2 peaks. The binding energy values are given with an error of ±0.2 eV, whereas the relative percentages of each component are given with an error of ±0.5%

| Sample name	O1s	Fe2p3/2	Sr3d5/2
Ce0	529.3 (55.2%) (O_L)	710.3 (84.7% Fe^{3+})	132.7 (100% Sr_L)
	531.8 (45.8%) (O_{OH})	712.6 (15.3% Fe^{4+})	
Ce5	529.2 (39.0%) (O_L)	709.7 (81.9% Fe^{3+})	133.1 (64.6% Sr_L)
	531.4 (61.0%) (O_{OH})	712.1 (18.1% Fe^{4+})	134.5 (35.4% $Sr_{OH/CO3}$)
Ce10	529.2 (38.7%) (O_L)	709.7 (83.3% Fe^{3+})	133.0 (84.8% Sr_L)
	531.6 (62%) (O_{OH})	712.1 (16.7% Fe^{4+})	134.3 (15.2% $Sr_{OH/CO3}$)
Ce15	529.3 (42.0%) (O_L)	709.7 (84.5% Fe^{3+})	132.9 (61.8% Sr_L)
	531.6 (58%) (O_{OH})	711.5 (15.5% Fe^{4+})	134.2 (38.2% $Sr_{OH/CO3}$)
MM	529.5 (58.8%) (O_L)	710.2 (88.1% Fe^{3+})	132.2 (82.1% Sr_L)
	531.8 (41%) (O_{OH})	712.3 (11.9% Fe^{4+})	133.9 (17.9% $Sr_{OH/CO3}$)
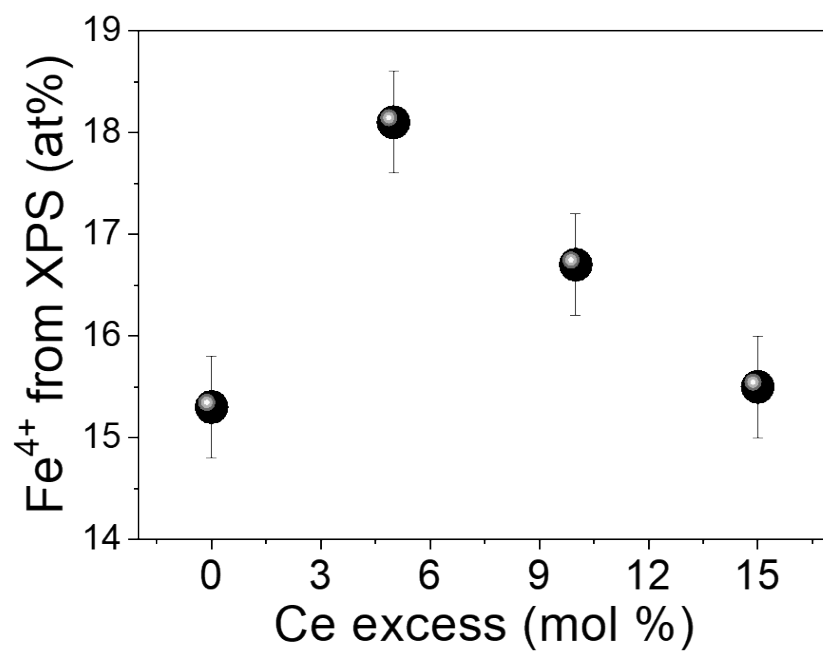
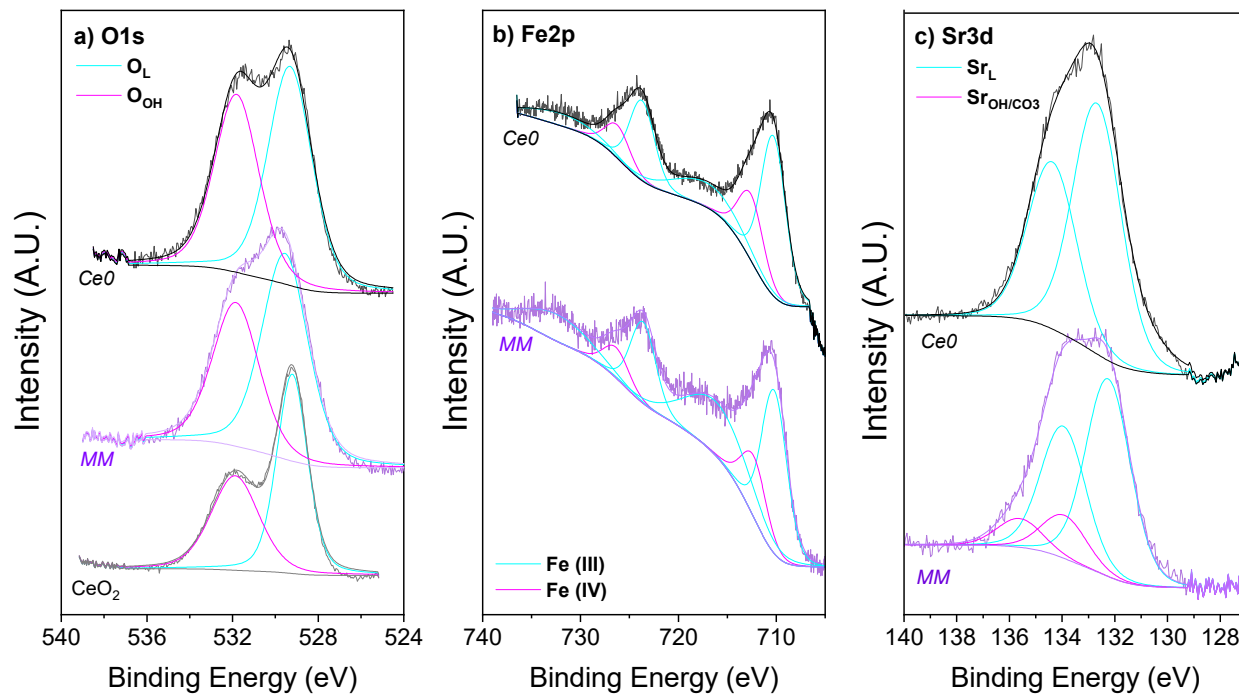**Figure S4. Trend of the Fe^{4+} calculated from XPS results (Table S2) with nominal cerium excess.**

Figure S5. X ray photoelectron Spectroscopy of *Ce0*, *MM* and CeO_2 samples: a) O1s region, b) Fe2p region and c) Sr3d region. O_L and O_{OH} represent the lattice oxygen and the surface oxygen, respectively, whereas Sr_L and $Sr_{OH/CO3}$ represent the Sr in the perovskite structure and the Sr in the $SrCO_3$ structure, respectively.

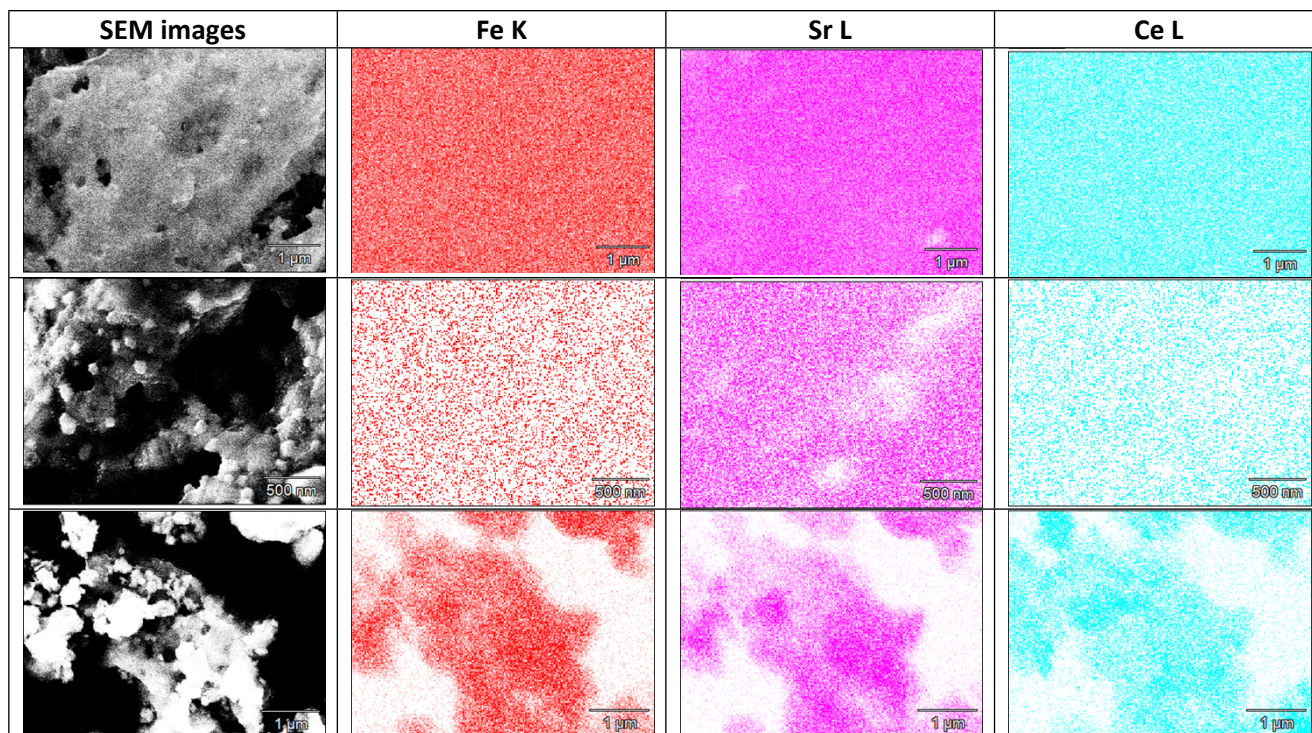| SEM images	Fe K	Sr L	Ce L

Figure S6. EDX mapping of *Ce0* (top row), *Ce15* (middle row), and *MM* (bottom row).
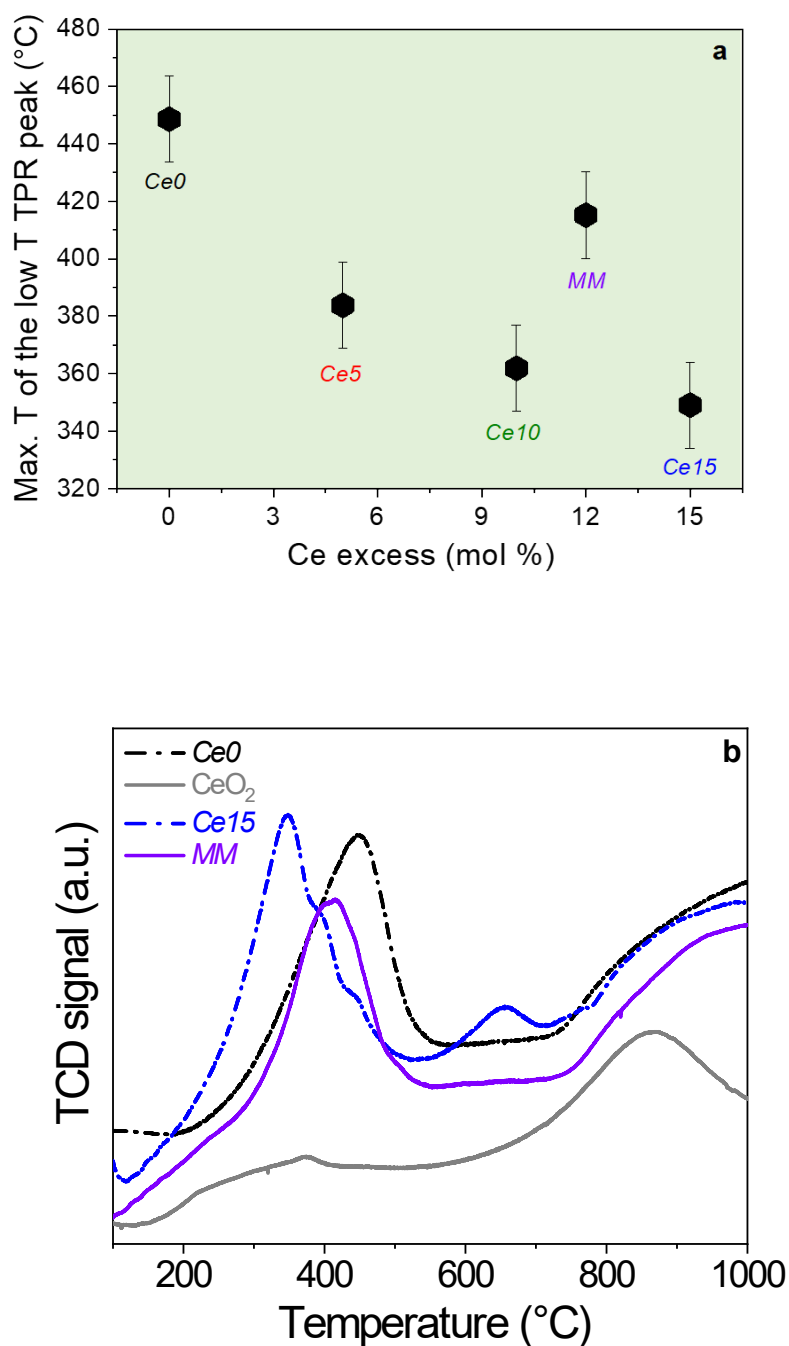
Figure S7. a) Trend of the maximum temperature (Tmax) of the low temperature TPR peak with cerium excess and comparison with the Tmax of *MM* sample; b) TPR profiles of *MM* and CeO₂ powders in comparison with *Ce0* and *Ce15*.

Discussion about TPR analysis of Figure 7

Figure S7 shows the TPR profiles of pure CeO_2 and of the mechanical mixture (*MM*) in comparison with *Ce0* and *Ce15*. For pure ceria reduction two main peaks at 375 and 870 °C where detected, that were

assigned to the surface and bulk reduction of CeO_2, respectively. Based on the H_2 consumption, the extent of ceria reduction (surface + bulk) was estimated as 73%. Based on the chemical composition of the *MM*, namely 89.4 wt.% of *Ce0* + 10.6 wt.% of CeO_2 and taking into account the extent of surface and bulk reduction of ceria only, the mmol H_2 g^{-1} that should be consumed for ceria were calculated (namely 0.0529 mmol g^{-1} for surface reduction and 0.1909 mmol g^{-1} for bulk reduction) and subtracting them from the consumption at low and high temperature, the H_2 uptake due to *Ce0* reduction in the low and temperature range, was estimated, while the H_2 consumption between 550-700 °C (0.28 mmol g^{-1}) was ascribed to the reduction of Ce^{4+} into the lattice of *Ce0*. There is a good correspondence between the reduction curve of the *MM* in comparison with those of *Ce0* and pure CeO_2. Briefly, the reduction profile of the *MM* appears as the result of the overlapping of the two reduction profiles, giving rise to a main reduction peak at relatively low T, at 415 °C that is an intermediate temperature between 375 and 450 °C. Such peak corresponds well to the surface ceria reduction along with to the reduction Fe^{4+} to Fe^{3+} in the *Ce0* sample. By increasing the temperature, between around 550-700 °C, reduction of Ce^{4+} present into the perovskite lattice occurs, then, reduction of ceria bulk (in the pure CeO_2 phase) and as well the reduction of Fe^{3+} to Fe^{2+} (in the perovskite *Ce0*), take place, both at around 800-1000 °C. Looking at **Table 2**, and comparing the H_2 uptake for *Ce15* and for the *MM*, the observed lower consumption (3.43 mmol H_2 g^{-1} for the *MM* versus 4.46 mmol H_2 g^{-1} for *Ce15*) is in agreement with the fact that in the *MM* sample pure ceria was introduced as a separated phase and not *in-situ* together with the perovskite precursors (as instead occurs for *Ce15*) and is reduced to a lower extent with respect to a defective ceria phase as it is formed in the case of *Ce15*. On the other hand, the crystallite size and surface area of pure CeO_2 phase and the one segregated in the *Ce15* can be different from the crystallite size determined by XRD (see **Table S1**), being the crystallite size of CeO_2 slightly smaller for the segregated samples compared to the pure CeO_2. This defective ceria that is reduced at about 650 °C might well correspond to the poorly crystallized nanostructured phase that was suggested from the structural characterization (see **Figure 1c**).
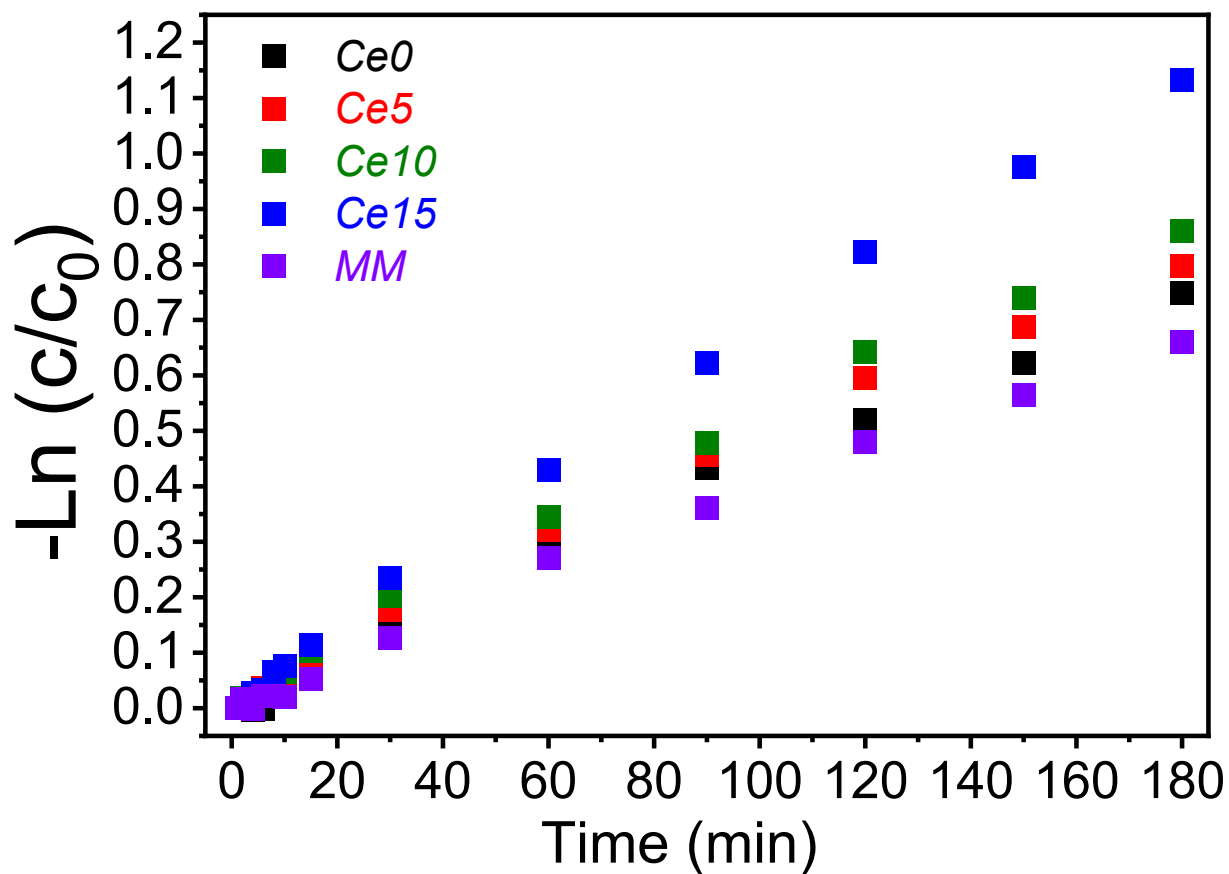
Figure S8. Linearized plots of the abatement of Bisphenol A using Ce-doped $SrFeO_3$ with different amount of cerium excess for calculation of kinetic constants